[O II] Hδ Hγ   Hβ   Hα

[O III] [O III]

GJ0641-5059

Flux mJy

Mg II   Hδ   Hγ

QJ0058-3337

Lyα   Si IV C IV   C III]

QJ0047-7530

C IV   C III]   Mg II
       Al III
                QJ0240-3434 A

                QJ0240-3434 B

Wavelength Angstroms

Figure 2.

redshift cluster), it clearly merits to be further studied, and monitoring is being attempted on the AAT.

GJ0641-5059: As its designation suggests, this emission-line galaxy was observed to be resolved and is not a QSO. However, it is still a remarkable object indeed. Its spectrum shows strong H Balmer lines, along with strong [O III], [Ne III], He I and [O II] – so much so that the continuum is almost invisible in the figure. All the lines are unresolved at 200 km/s. An examination of the line ratios shows the system to be a H II galaxy (rather than an AGN – Veilleux & Osterbrock, 1987). However, its extraordinarily high [O III]λ5007/Hβ ratio, places it among the most highly excited of such systems known.

Conclusion

We have found that standard QSO survey techniques can be efficiently applied to search for QSOs in arbitrary locations – i.e. behind nearby galaxies. Once such inertial reference objects have been identified, astrometric programmes targeted at these galaxies can be commenced with the NTT. In fact, the NTT will be extremely well placed to commence these programmes later this year, when service mode operations begin after its re-commissioning, since service mode observing offers the best chance of obtaining images in the excellent seeing conditions essential for these high-precision astrometric observations.

References

Lynden-Bell, D. & Lynden-Bell, R.M., 1995, MNRAS, **275**, 429.
Majewski, S.R., 1994, ApJ, **431**, L17.
Tinney, C.G., 1993, The Messenger, **74**, 16.
Tinney, C.G., 1995, MNRAS, **277**, 609.
Tinney, C.G., Da Costa, G. & Zinnecker, H., 1996, MNRAS, submitted.
Veilleux, S. & Osterbrock, D.E., 1987, ApJS, **63**, 295.

E-mail address: Chris Tinney,
cgt@aaoepp.aao.gov.au

A Multiline Molecular Study of the Highly Collimated Bipolar Outflow Sandqvist 136

G. GARAY [1], I. KÖHNENKAMP [1] and L.F. RODRIGUEZ [2]

1 Departamento de Astronomía, Universidad de Chile, Chile
2 Instituto de Astronomía, Universidad Nacional Autónoma de México, México

Introduction

Following the discovery of bipolar molecular outflows in the earliest 80's (Snell, Loren & Plambeck, 1980; Rodríguez, Ho & Moran, 1980), a wealth of observations have shown that this phenomenon is commonly detected in star-forming regions. During their earliest phase of evolution stellar objects are thought to generate a fast, well collimated bipolar wind that sweeps up the am-
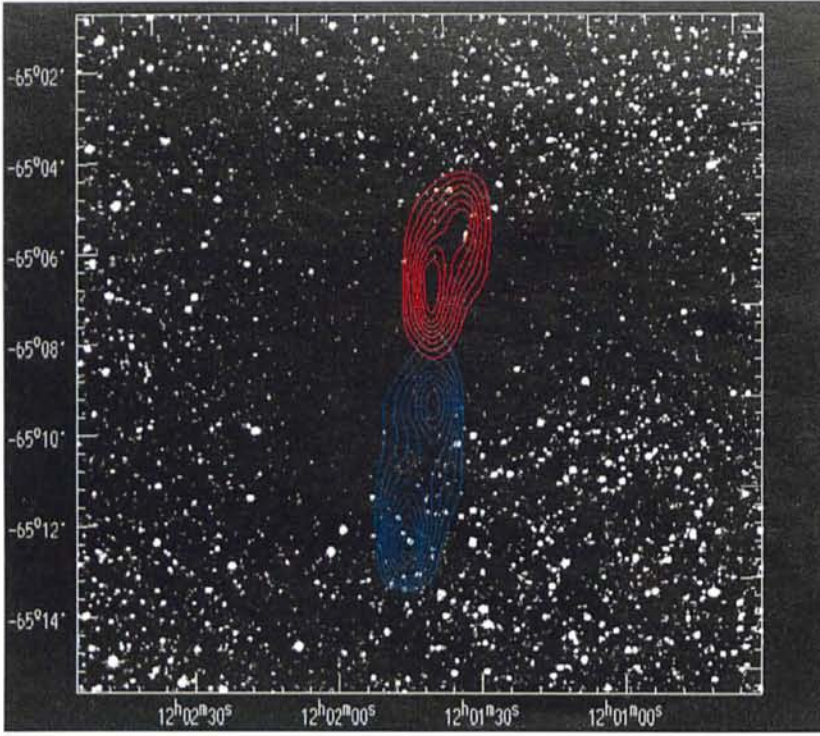
31

Figure 1: Contour map of velocity integrated CO(1→0) line wing emission from the Sandqvist 136 bipolar outflow, superimposed on a V-band image of the globule taken from the Digitised Sky Survey. Co-ordinate labels are J2000. Blue contours correspond to the emission integrated in the velocity range from −13.5 to −8.5 km s⁻¹ (blueshifted wing) and red contours to the integrated emission in the velocity range from −0.5 to 4.5 km s⁻¹ (redshifted wing). The lowest contour and contour interval are, respectively, 1.8 and 0.8 K km s⁻¹ for the redshifted emission and 1.0 and 0.5 K km s⁻¹ for the blueshifted emission.

bient gas in its vicinity, giving rise to the molecular outflows. Bipolar flows are frequently found associated with other tracers of the dynamical interaction between the high-velocity wind and ambient gas, such as Herbig-Haro objects (Reipurth, 1991), shock-excited infrared H₂ emission (Bally, Lada & Lane, 1993), and optical jets (Mundt, 1988). Reviews of the characteristics of bipolar molecular outflows have recently been presented by Bachiller & Gómez-González (1992) and Fukui et al. (1993). The majority of the outflows show a moderate degree of collimation, while few have highly colli-
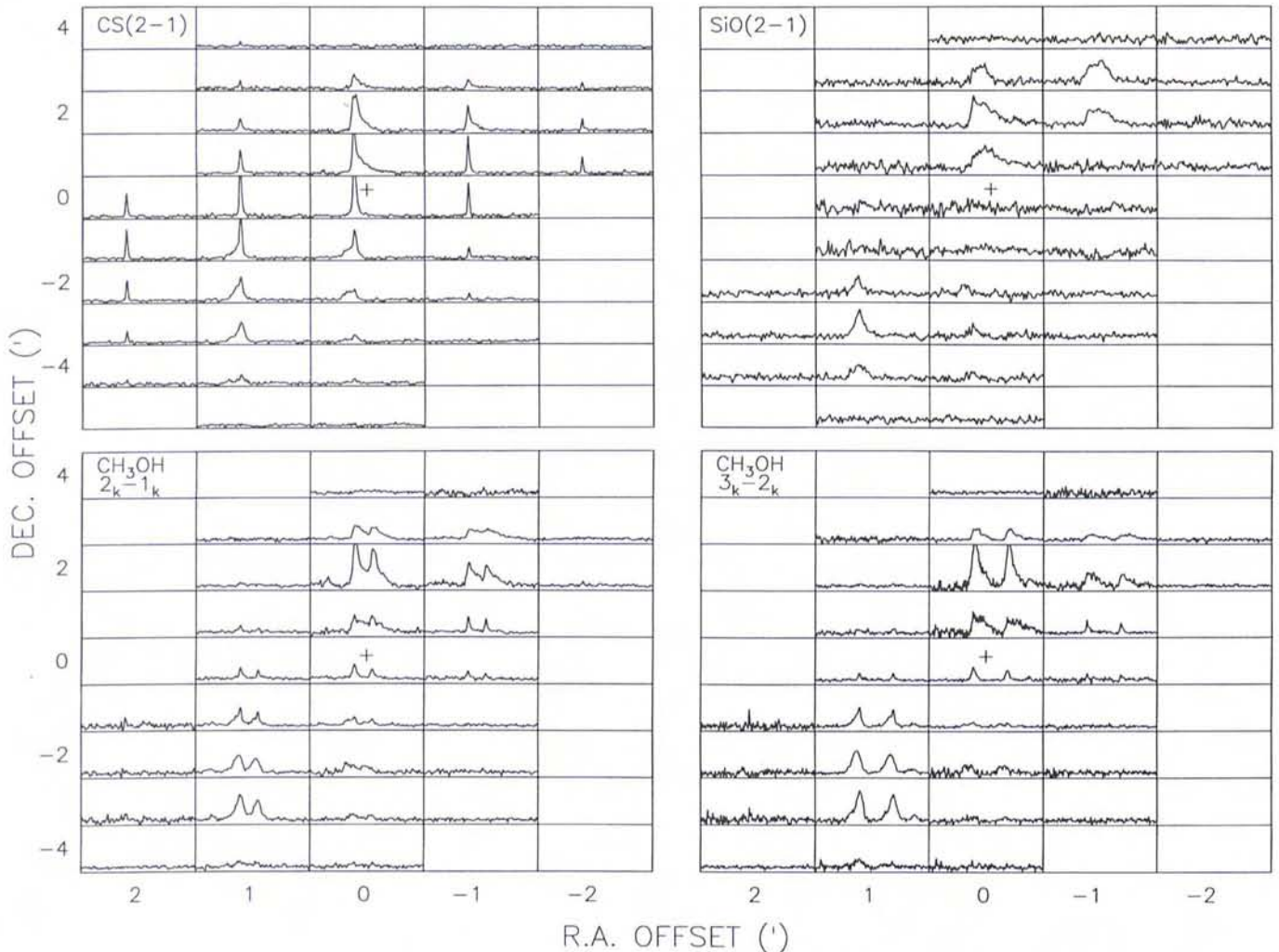

Figure 2. Observed spectra across the 5′× 10′central region of the Sandqvist 136 globule. The grid spacing is 1′. Offsets are from the reference position at α = 11ʰ59ᵐ1.2ˢ and δ = −64°52′0″. In each box the velocity scale ranges from −20 to 20 km s⁻¹. Upper left: CS(2→1) emission. Antenna temperature scale: −0.1 to 1.5 K. Upper right: SiO(2 →1) emission. Antenna temperature scale: −0.1 to 0.4 K. Bottom left: CH₃OH(2ₖ → 1ₖ) emission. Antenna temperature scale: −0.2 to 1.8 K. Bottom right: CH₃OH(3ₖ → 2ₖ) emission. Antenna temperature scale: −0.2 to 1.8 K. The cross indicates the position of the IRAS source 11590-6452.

mated bipolar morphologies (André et al., 1990; Bachiller et al., 1990; Bachiller, Fuente & Tafalla, 1995; Lada & Fich, 1996). The class of highly collimated outflows are thought to be driven by jets that accelerate the ambient gas through the propagation of shocks (e.g. Raga & Cabrit, 1993).

The interaction of high-velocity jets from young stars with the surrounding ambient gas generates strong shock waves which are expected to produce a significant transformation of the physical properties of the molecular surroundings as well as of its chemical composition. Although there has been a substantial amount of work on the physical characteristics of outflows, very little is known about their chemical composition. Basic questions such as: How is the chemistry of the swept-up ambient molecular material affected by the winds from young stellar objects? or Do molecular abundances serve as sensitive probes of the evolutionary stage of bipolar outflows? (cf. van Dishoeck & Blake, 1995) have not yet been answered. Shocks in dense molecular clouds are expected to radiate in several molecular lines in the millimetre and submillimeter wavelength ranges and hence are open to investigation by spectroscopic observations at these wavelengths. Since different molecules and their isotopes respond differently to physical conditions (such as temperature and density) their observations provide unique tools to probe the outflows. Mapping outflows in different molecular species is thus essential to the study of the physical and chemical structure of the shocks.

Most of the studies of molecular outflows from young stellar objects have focused, to a large extent, on observations of the CO(1→0) line (Bally & Lada, 1983; Lada, 1985). Emission in this transition is easy to detect, both due to the relatively large abundance of CO and easy excitation at the densities and kinetic temperatures of molecular flows. Very few multiline mapping of molecular outflows have been performed so far. Part of the reason, other than the usual constraint on observing time, is that observations in the range of wavelengths that permit us to probe abundances in outflows have been made available only recently. In particular the Swedish-ESO Submillimetre Telescope (SEST) has recently undergone important upgrade in the receiver front end, opening the 2-mm wavelength range for observations and substantially improving the performance in the 3-mm wavelength range. In these ranges, emission from a plethora of molecular lines is expected to be detectable, which can be used to trace the motions and physical conditions of the gas at the earliest stages of star formation. Accordingly, the SEST has opened the avenue for a detailed investigation of the chemical composition of southern skies outflows, which would undoubtedly provide
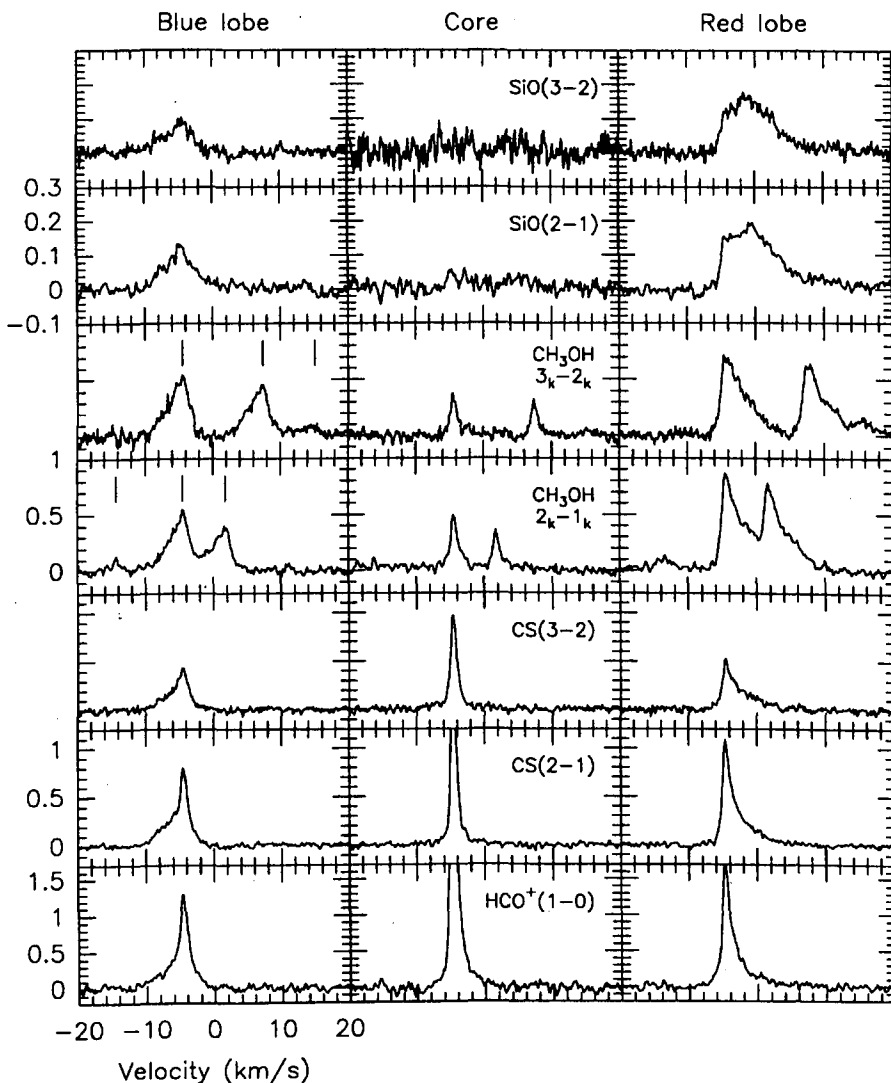

Figure 3. Spectra of the spatially integrated line emission from the blue and red lobes of the Sandqvist 136 outflow and from the central position (Middle column).

much-needed information about their physical and chemical evolution.

Sandqvist 136 (Sandqvist, 1977) is a small dark cloud or Bok globule, located at a distance of ~175 pc from the Sun, which harbours a highly collimated bipolar outflow near its centre (Bourke et al., 1996; see Figure 1) The CO outflow is found to be well described as a biconical flow, with a semi-opening angle of 15° and inclined from the line of sight by an angle of ~ 84°, in which the gas moves outwards with a constant radial velocity (with respect to the cone apex) of ~ 28 km s^{-1}. The outflow appears to be driven by a very young stellar object, with a luminosity of ~ 7 $L_\odot$, possibly still undergoing accretion of matter. Its characteristics at infrared and millimetre wavelengths are similar to those of Class 0 objects (André, 1995). Since the lobes of this outflow extend by ~ 4' in the plane of the sky it is an ideal source for a detailed study, using single-dish instruments, of the physical and chemical characteristics across highly collimated, low velocity shocks. In this article we report extensive molecular SEST observations of this out-

flow in rotational transitions of silicon monoxide (SiO), methanol (CH$_3$OH), carbon monosulfide (CS), and formyl ion (HCO$^+$).

Observations

The observations of the Sandqvist 136 outflow, stimulated by the recent availability at the 15-m SEST radio telescope of sensitive SiS receivers operating in the 2- and 3-mm bands, were performed during September 1995. We used the 2- and 3-mm receivers to simultaneously observe the J = 3 → 2 and J = 2 → 1 transitions of CS, the J = 3 → 2 and J = 2 → 1 transitions of SiO, and some of the $J_k = 3_k → 2_k$ and $J_k = 2_k → 1_k$ transitions of CH$_3$OH. Single-sideband receiver temperatures were typically 120 K for both receivers. As backend we used high-resolution acousto-optical spectrometers providing a channel separation of 43 KHz and a total bandwidth of 43 MHz. This resulted in spectral resolutions of 0.13 and 0.09 km s^{-1} and total velocity coverages of 133 and 89 km s^{-1} at the 96.7 and 145.1 GHz frequencies of the CH$_3$OH lines, respec-
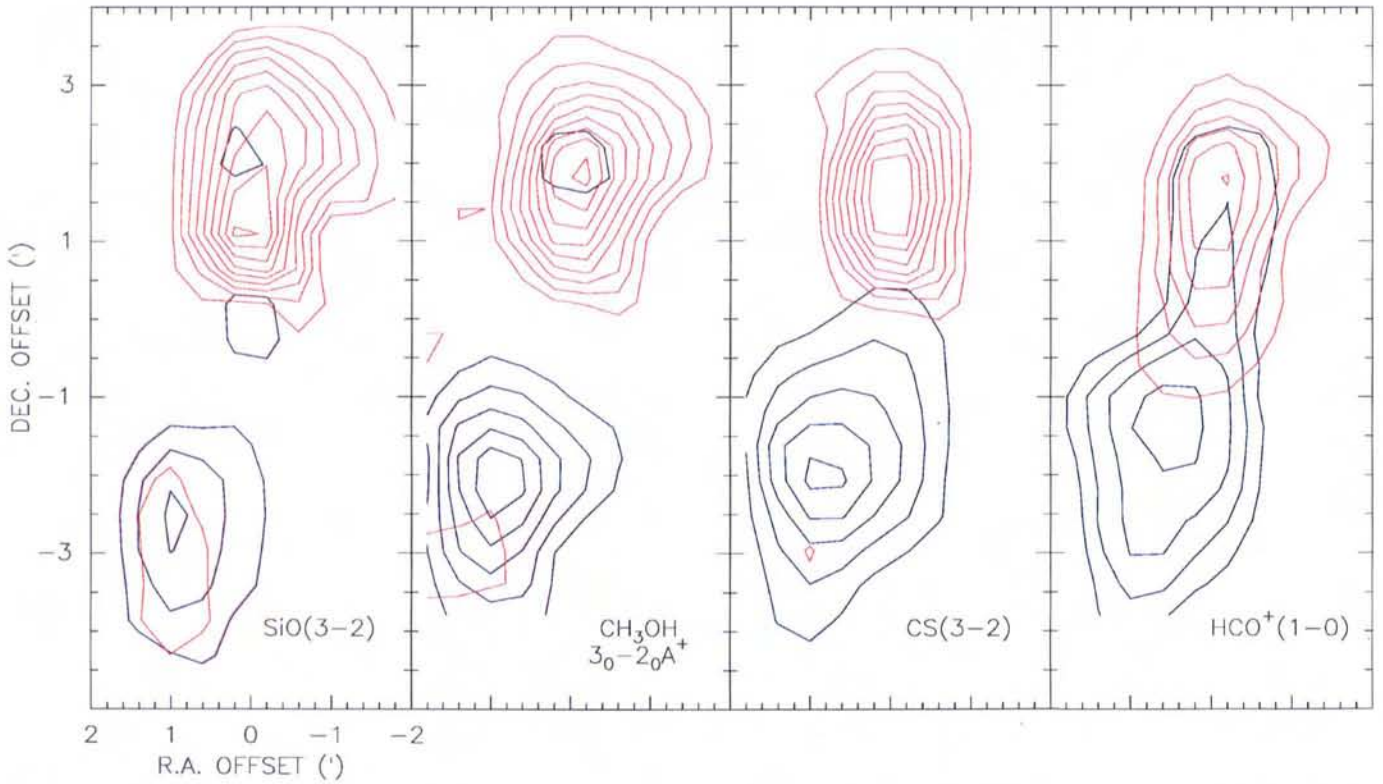
V_{blue}: -9.1 to -5.5 km s^{-1} V_{red}: -3.1 to 0.5 km s^{-1}

Figure 4. Contour maps of velocity integrated line wing emission from the Sandqvist 136 bipolar outflow. Blue contours correspond to the emission integrated in the velocity range from -9.1 to -5.5 km s^{-1} (blueshifted wing) and red contours to the integrated emission in the velocity range from -3.1 to 0.5 km s^{-1} (redshifted wing). The lowest contour and contour interval are, respectively, 0.1 and 0.1 K km s^{-1} for the SiO($J = 3 \rightarrow 2$) line (left), 0.3 and 0.3 K km s^{-1} for the CH$_3$OH($3_0 \rightarrow 2_0$)A$^+$ line (middle-left), 0.2 and 0.15 K km s^{-1} for the CS($J=3 \rightarrow 2$) line (middle-right), and 0.4 and 0.3 K km s^{-1} for the HCO$^+$($J=1 \rightarrow 0$) line (right).

tively. Within the available bandwidths, three rotational transitions of CH$_3$OH could be observed at 2 mm ($3_0 \rightarrow 2_0$A$^+$, $3_{-1} \rightarrow 2_{-1}$E, and $3_0 \rightarrow 2_0$E lines) and three at 3 mm ($2_0 \rightarrow 1_0$E, $2_0 \rightarrow 1_0$A$^+$, and $2_{-1} \rightarrow 1_{-1}$E lines). The antenna half-power beam width and main beam efficiency were, respectively, 34″ and 0.66 at the highest observed frequency of 147 GHz and 57″ and 0.75 at the lowest observed frequency of 87 GHz. In each transition, we mapped the molecular emission within a region of ~ 5′ × 10′, with 60″ spacings. All the observations were performed in the position switch mode. The integration times on source were typically 3 minutes per position.

Results

The spectra in the $J = 2 \rightarrow 1$ lines of CS and SiO and in the $J_k = 2_k \rightarrow 1_k$ and $J_k =$ $3_k \rightarrow 2_k$ lines of CH$_3$OH observed across the 5′ × 10′ region mapped with SEST are shown in Figure 2. Two emission components, originating from physically and chemically different environments, can be distinguished from this figure. A narrow line emission, at a velocity of -4.5 km s^{-1}, arising from the ambient cloud material at the core of the Sandqvist 136 globule (see upper left panel), and a broad line emission which arises from the bipolar outflowing gas. Particularly striking are the cases of methanol and silicon monoxide molecules, in which the emission from the broad component is much stronger than in the narrow component. The broad emission is detected at redshifted velocities with respect to the systemic ambient cloud velocity toward the northwest region of the map (the red lobe) and at blueshifted velocities toward the southeast region (the blue lobe).

Figure 3 shows the spectra of the spatially integrated line emission, in all the observed transitions, from both the blue and red lobes as well as from the central core position. Emission in the lines of SiO is found to arise only from the lobes, no emission being detected at the core of the globule. The CH$_3$OH profiles show strong emission from the broad component and weak emission from the narrow ambient cloud, while the CS and HCO$^+$ profiles show a mixture of strong emission from the quiescent ambient cloud and relatively weaker wing emission at the position of the lobes. The vertical bars shown in the spectra of methanol indicate the expected positions of the three rotational transitions, within the observed velocity ranges, for a rest velocity of -4.5 km s^{-1}. Wing emission is detected in all the observed molecules: CS, SiO, HCO$^+$ and CH$_3$OH. Maps of the velocity integrated emission

TABLE 1. Derived Parameters of Sandqvist 136 Outflowing Gas

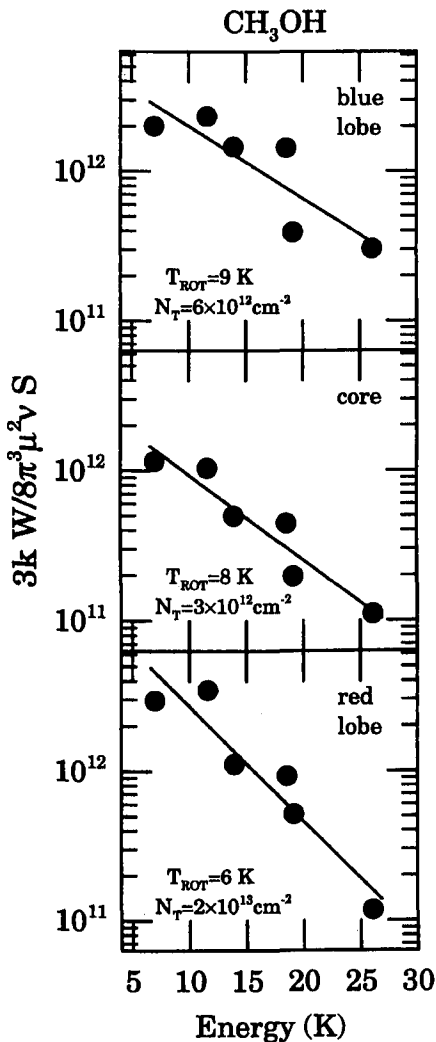| Offset pos.		Wing	CH$_3$OH		SiO		CS		HCO$^+$
$\Delta\alpha$ (′)	$\Delta\delta$ (′)		T_R (K)	N_T (cm^{-2})	T_R (K)	N_T (cm^{-2})	T_R (K)	N_T (cm^{-2})	N_T (cm^{-2})
1	-3	Blue	6	2.4×10^{14}	9	7.6×10^{11}	6	6.7×10^{12}	9.2×10^{11}
1	-2	Blue	9	1.7×10^{14}	9	6.2×10^{11}	8	5.7×10^{12}	1.0×10^{12}
0	2	Red	6	6.2×10^{14}	8	2.2×10^{12}	7	1.3×10^{13}	2.0×10^{12}
-1	2	Red	6	4.3×10^{14}	6	1.8×10^{12}	6	1.2×10^{13}	8.8×10^{11}

CH₃OH

Figure 5. Rotation diagrams for the methanol transitions observed toward the red lobe, central core, and blue lobe of Sandqvist 136. The lines correspond to least squares linear fits to the observed data. The derived values of the rotational temperature and total column density are given in the lower left corner.

in the blue and red wings of the SiO(3→2), CH₃OH(3₀→2₀)A⁺, CS(3→2), and HCO⁺(1→0) lines are shown in Figure 4. These maps show that the spatial distribution of the wing emission from the Sandqvist 136 bipolar outflow is similar in all the observed molecular species. The emission peaks of the blue and red lobes are offset by ~ 4′ or 0.2 pc from each other with a position angle of ~ −12°.

Since at least two rotational lines of the CS, SiO, and CH₃OH molecules were observed simultaneously, we performed rotational diagram analysis in order to derive their rotational temperature, T_{rot}, and total column density, N_T. In this method these parameters are derived from a fit to the relationship between the quantity $3 k \int T_{mb} dv / 8\pi^3 \mu^2 \nu S$ and the energy of the upper level of the transition. Here μ, ν, and S are the transition dipole moment, frequency, and line strength of the transition, respectively, and $\int T_{mb} dv$ is the velocity integrated main beam brightness, obtained directly from the observa-

tions. In Table 1 we give the derived rotational temperatures and column densities of CS, CH₃OH and SiO in selected positions of the red and blue lobes of the outflow. For the blue lobe we integrated the emission in the LSR velocity range from −9.3 to −5.3 km s⁻¹, while for the red lobe we integrated the emission in the LSR velocity range from −3.7 to 0.3 km s⁻¹. As a mode of illustration we show in Figure 5 a sample of the data used for the derivation of the parameters associated with the CH₃OH molecule. Plotted are data obtained at three positions within the Sandqvist globule: blue lobe, red lobe, and central core position. The rotational temperature and total methanol column density derived from a linear least squares fit to these data are shown in the lower left corner. The derived rotational temperatures of the outflowing gas at the lobes and of the quiescent gas at the core position are all similar, with an average value of 8 K and a dispersion of 2 K. Further, there is no significant differences among the rotational temperatures derived using different molecular species. These temperatures are somewhat lower than the kinetic temperature derived for the quiescent dark cloud of 13 K (Bourke *et al.*, 1995). Whether the rotational temperatures provide a good estimate of the kinetic temperature of the outflowing gas is not clear. Bachiller *et al.* (1995) suggest that the methanol populations are likely to be extremely sub-thermal and therefore that the rotational temperatures are considerably smaller than the kinetic temperatures.

The abundance of species X relative to CO, [X]/[CO], of the outflowing gas in the lobes of Sandqvist 136 are given in Table 2. They were directly derived as the ratio of the molecular column density of species X, obtained from the rotational analysis (see Table 1), and the column density of CO molecules in the corresponding velocity range. The latter was computed from the ratio of the observed emission in the ¹²CO and ¹³CO lines assuming a ¹²CO/¹³CO ratio of 89 and an excitation temperature of 8 K (see Bourke *et al.*, 1996 for a description of the method). Since for the Sandqvist 136 cloud the ambient gas and shocked gas are well distinguishable, both spatially and kinematically, the derived abundances of the outflowing gas are not affected by the emission of the quiescent gas.

Discussion

The data presented in the previous section clearly illustrate that the chemistry of the molecular gas near the core of the globule has been substantially modified as a result of the interaction between the shocks and the ambient medium. Particularly notable are the strong emission in the lines of methanol and silicon monoxide at the position of the lobes, showing that these species are dramatically affected by the shocks. To quantitatively assess the chemical changes of the ambient medium due to the outflow phenomena requires to know the chemical abundances of the quiescent ambient gas. These have not yet been determined for the Sandqvist 136 globule. We note that the spectra observed toward the central position of the core region reflect the conditions of the dense molecular gas that surrounds the recently formed star, with a possible contribution from a circumstellar disk, and thus they do not probe the chemical state of the large scale ambient medium. We will assume that the abundances of the Sandqvist 136 quiescent ambient cloud are similar to those of cold dark clouds which show no evidence of star formation, such as the TMC-1 ridge and the L134N cloud (see van Dishoeck *et al.*, 1993, and references therein). The [X]/[CO] abundance ratios in the TMC-1 dark cloud are given in column 4 of Table 2. A comparison of columns 2, 3 and 4 of Table 2, shows that the [CH₃OH]/[CO] and [SiO]/[CO] abundance ratio in the lobes of the Sandqvist 136 outflow have been enhanced with respect to that of the quiescent ambient gas in dark globules by factors of ~200 and ~1000, respectively.

The spatial distribution of the emission in the SiO and CH₃OH lines and their spectacular enhancement with respect to that of the ambient medium shows that shocks play an essential role in the production of these molecules. The formation route of these species by the action of shocks is twofold: via gas phase and via grain surface processes. Shocks can raise the gas to high temperatures and drive many chemical reactions which are inefficient at ambient cloud temperatures. Shocks can also partially destroy dust grains leading to the injection of several absorbed atoms and molecules from the grain surface into the gas phase. Whether the high abundance of silicon monoxide and methanol molecules seen

TABLE 2. Molecular Abundances Relative to CO.

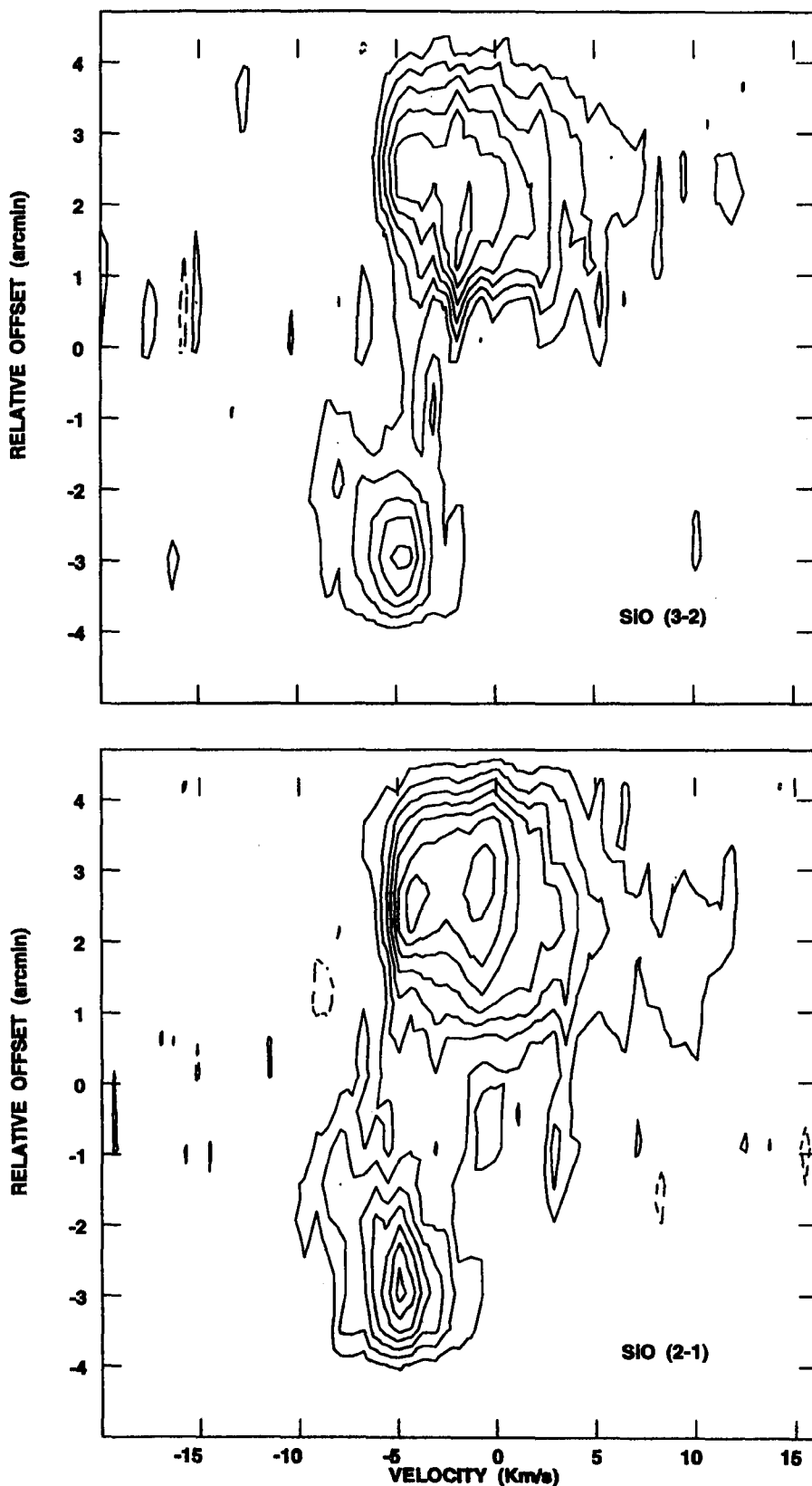| Molecule	Sandqvist 136		TMC-1
	blue lobe	red lobe	
CH₃OH	4×10^{-3}	8×10^{-3}	2.5×10^{-5}
SiO	1×10^{-5}	3×10^{-5}	$< 2.5 \times 10^{-8}$
CS	1×10^{-4}	2×10^{-4}	1.3×10^{-4}
HCO⁺	2×10^{-5}	2×10^{-5}	1.0×10^{-4}

Figure 6. Position-velocity diagram of the SiO emission along the symmetry axis of the outflow. Top: SiO(3 →2). Contour levels are { −1, 1, 2, 3, 4, 5 and 6} × 0.030 K. Bottom: SiO(2 →1). Contour levels are { −1, 1, 2, 3, 4, 5, 6 and 7} × 0.0275 K.

Dalgarno, 1977; Hartquist, Oppenheimer & Dalgarno, 1980). Models of the chemistry in regions behind fast dissociative shocks predict a substantial enhancement in the abundance of SiO molecules (Neufeld & Dalgarno, 1989). In particular, for shocks with velocities of 60–80 km s^{-1} propagating in a gas with pre-shock density of 10^4 cm^{-3} (about the density of the Sandqvist 136 globule of 5×10^3 cm^{-3}; Bourke et al., 1996) the predicted column densities of SiO molecules are $\sim 2 - 4 \times 10^{12}$ cm^{-2}, similar to those derived in the lobes of the Sandqvist flow. A possible drawback with dissociative shock models is that the predicted temperatures of the post-shock gas are high ($\sim$ 200 K), while the derived rotational temperatures are an order of magnitude smaller. Since the post-shock temperature in C shocks are much lower than in J shocks of the same speeds, the former type of shocks would appear as most promising to explain the observed characteristics of the Sandqvist flow. In particular the synthesis of molecules from atoms and ions can be highly efficient behind non-dissociative C-type shocks. The detection of profuse SiO emission from other highly collimated bipolar outflows have been reported by Bachiller, Martín-Pintado & Fuente (1991), Mikami et al. (1992), Martín-Pintado et al., (1995), and Zhang et al. (1995).

The large [CH$_3$OH]/[CO] abundance ratio of the outflowing gas in the Sandqvist lobes, greater than in quiescent dark clouds by factors of $\sim$ 200, can not be explained by gas phase chemistry alone (Millar, Herbst & Charnley, 1991). Similar enhancements in the abundance of methanol in other young bipolar outflows have been reported by Bachiller et al. (1995). The large increase in the CH$_3$OH abundance is most likely the result of desorption from dust grains due to shocks (Charnley, Tielens & Millar, 1992). Refractory grains are likely to be surrounded by icy grain mantles, whose compositions depend on the physical conditions of the ambient medium. Molecules such as H$_2$O and CH$_3$OH are expected to dominate in atomic hydrogen-rich ambient medium such as that of molecular clouds. Shocks can raise the temperature of the gas evaporating the icy organic mantles of the grains and returning these material to the gas phase.

We also find that the [HCO$^+$]/[CO] abundance ratio of the outflowing gas in Sandqvist 136 is smaller than in quiescent dark clouds by a factor of $\sim$ 5. Theoretical models of gas phase chemistry behind shocks predict that the abundance of molecules such as HCO$^+$, CN, and H$_2$CO should decrease with respect to the pre-shock abundances (Iglesias & Silk, 1978; Mitchell, 1987). For instance, theoretical calculations of a 10 km s^{-1} shock propagating into a cloud with a pre-shock density of 10^4 cm^{-3}, show that

toward the Sandqvist 136 outflow are produced in the gas-phase shock chemistry or released directly from the dust grains by shock evaporation remains to be investigated.

The high abundance of SiO molecules is most likely due to the injection into the gas phase, by shocks, of Si from a population of refractory grains which are composed of silicates and graphites. Once silicon is injected into the gas phase, chemical models based on ion-molecule reactions predict a large abundance of SiO molecules (Turner &

the abundance of HCO$^+$ decreases by a factor of ~ 20 (Iglesias & Silk, 1978). The derived [HCO$^+$]/[CO] ratios in the lobes of Sandqvist 136 then give further support to the notion that the abundances in the lobes are a product of shock chemistry.

In addition to the wing emission detected toward the lobes of Sandqvist 136 in the lines of SiO and CH$_3$OH, we note the presence of emission at velocities comparable to the systemic velocity of the globule. In particular for silicon monoxide, emission in the velocity range of the ambient cloud is observed only at the position of the lobes. This can be appreciated in Figure 6 which shows velocity-position diagrams of the emission in the SiO lines along the symmetry axis of the outflow. The strength of the emission in the red lobe is roughly constant with velocity, with peaks at −4.1 and −0.8 km s^{-1}, while in the blue lobe the emission peaks at a velocity of −5.0 km s^{-1}, close to the ambient cloud velocity. This result suggests that the enhancement of SiO and CH$_3$OH molecules might be due to two different processes: heating of grains within the ambient core medium by the UV radiation produced in the shocks, which can evaporate volatile grain mantles and trigger gas-phase reactions, and direct shock processing of dust located within the shocked region. The low velocity emission would then arise from pre-shock gas heated by the radiation from the hot post-shock gas, while the high velocity emission arises from the cold post shock gas.

Conclusions and Outlook

Multiline molecular observations toward the Sandqvist 136 dark globule have revealed a spectacular enhancement in the abundance of silicon monoxide and methanol molecules at the lobes of the associated bipolar outflow. The spatial distribution and broad line profiles of the SiO and CH$_3$OH emission indicates a common mechanisms for the excitation of these lines: shocks. We conclude that the shocks created by the interaction between flows and the surrounding medium play a major role in the production of these molecules. In partic-

ular the strong emission observed in the methanol lines suggest that these lines can be used as powerful signposts of the chemical impact of bipolar outflows on the surrounding ambient medium. It appears that the Sandqvist 136 shock produces the evaporation of icy grain mantles resulting in the injection into the gas phase of large amount of ice mantle constituents, such as methanol. Further, the shock seems to be sufficiently powerful that refractory dust grains are partially destroyed, liberating into the gas phase a significant amount of Si atoms that are later converted to SiO by ion-molecule reactions and/or shock chemistry. Finally, we find that the SiO and CH3OH emission detected toward the lobes not only traces shocked outflowing gas but also ambient medium gas that has been heated by the UV radiation from the hot post shock regions.

It has been suggested that the strength of the emission in diverse trace molecules might be considered an indicator of the evolutionary stage of bipolar outflows (Bachiller & Gómez-González, 1992). It would appear that the profuse emission observed in the lines of methanol and silicon monoxide from the Sandqvist 136 outflow implies that we are witnessing an early stage of the outflow phase in which molecules in icy mantles and atoms in dust grains are efficiently liberated back into the gas phase. How much of the enhancement factor depends on wind velocity and/or on evolutionary age has not, however, yet been established. The determination of the abundance of more complex organic molecules in the lobes, such as CH$_3$OCH$_3$, HCOOCH$_3$, and CH$_3$CN, which can potentially serve as clocks of the evolutionary state of the outflows (van Dishoeck & Blake, 1995), should be obtained to provide answer to these questions.

References

André, P. 1995, *Astr. & Spa. Sci.* 224, 29.
André, P., Martín-Pintado, J., Despois, D., & Montmerle, T. 1990, *A&A* 236, 180.
Bachiller, R., Cernicharo, J., Martín-Pintado, J., Tafalla, M., & Lazareff, B. 1990, *A&A* 231, 174.
Bachiller, R., Fuente, A., & Tafalla, M., 1995, *ApJ* 445, L51.
Bachiller, R., & Gómez-González, J. 1992, *A&AR* 3, 257.
Bachiller, R., Liechti, S., Walmsley, C.M., & Colomer, F. 1995, A&A 295, L51.
Bachiller, R., Martín-Pintado, J., & Fuente, A. 1991, *A&A* 243, L21.
Bally, J., & Lada, C.J. 1983, *ApJ* 265, 824.
Bally, J., Lada, E., & Lane, A.D. 1993, *ApJ* 418, 322.
Bourke, T.L., Garay, G., Lehtinen, K.K., Köhnenkamp, I., Launhardt, R., Nyman, L.-A., May, J., Robinson, G., & Hyland, A.R. 1996, *ApJ* submitted.
Bourke, T.L., Hyland, A.R., Robinson, G., James, S.D., & Wright, C.M. 1995, *MNRAS* 276, 1067.
Charnley, S.B., Tielens, A.G.G.M., & Millar, T.J. 1992, *ApJ* 399, L71.
Fukui, Y., Iwata, T., Mizuno, A., Bally, J., & Lane, A.P. 1993, in *Protostars and Planets III*, eds. E.H. Levy & J. Lunine (Tucson: Univ. Arizona Press), 603.
Lada, C.J. 1985, *ARA&A* 23, 267.
Lada, C.J., & Fich, M. 1996, *ApJ* in press.
Hartquist, T.W., Oppenheimer, M., & Dalgarno, A. 1980, *ApJ* 236, 182.
Iglesias, E.R. & Silk, J. 1978, *ApJ* 226, 851.
Martín-Pintado, J., Bachiller, R., & Fuente, A. 1992, *A&A* 254, 315.
Mikami, H., Umemoto, T., Yamamoto, S., & Saito, S. 1992, *ApJ* 392, L87.
Millar, T.J., Herbst, E., & Charnley, S.B. 1991, *ApJ* 369, 147.
Mitchell, G.F. 1987, in Astrochemistry, IAU Symposium No. 120, 275.
Mundt, R. 1988, in *Formation and Evolution of Low Mass Stars*, eds. A.K. Dupree and M.T.V.T. Lago, 257.
Neufeld, D.A., & Dalgarno, A. 1989 *ApJ* 340, 869.
Raga, A., & Cabrit, S. 1993, *A&A* 278, 267.
Reipurth, B. 1991, in *The Physics of Star Formation and Early Stellar Evolution*, eds. C.J. Lada and N.D. Kylafis, 497.
Rodríguez, L.F., Ho, P.T.P., & Moran, J.M. 1980 *ApJ* 240, L149.
Sandqvist, A. 1977, *A&A* 57, 467.
Snell, R.L., Loren, R.B., & Plambeck, R.L. 1980, *ApJ* 239, L17 .
Turner, J.L., & Dalgarno, A. 1977, *ApJ* 213, 386.
van Dishoeck, E.F. & Blake, G.A. 1995, *Astr. & Spa. Sci.* 224, 237.
van Dishoeck, E.F., Blake, G.A., Draine, B.T., & Lunine, J.I. 1993, in *Protostars and Planets III*, eds. E.H. Levy & J.I. Lunine (Tucson: Univ. Arizona Press), 163.
Zhang, Q., Ho, P.T.P., Wright, M.C.H., & Wilner, D.J. 1995, *ApJ* 451, L71.

E-mail address:
guido@calan.das.uchile.cl (Guido Garay)

On the Optical Emission of the Crab Pulsar

E.P. NASUTI[1, 3], *R. MIGNANI*[1], *P.A. CARAVEO*[1] *and G.F. BIGNAMI*[1, 2]

[1]*Istituto di Fisica Cosmica del CNR, Milan, Italy;* [2]*Dipartimento di Ingegneria Industriale, Università di Cassino, Italy;* [3]*Università degli Studi di Milano, Italy*

1. Introduction

The Crab Pulsar (PSR0531 +21) was the first Isolated Neutron Star (INS) de-tected at optical wavelengths. It is identi-fied with a star (V ~ 16.5) near the cen-tre of the Crab Nebula, the remnant of the supernova explosion observed in the summer of 1054. The identification has been confirmed by the discovery of pulsed optical emission at the radio peri-od (Cocke et al., 1969).